Springer

KSME

Journal of Mechanical Science and Technology 30 (9) (2016) 3907~3915
www.springerlink.com/content/1738-494x(Print)/1976-3824(Online)
DOI 10.1007/s12206-016-0802-5

Effect of surface conditions on blast wave propagation †

Seungho Song[1], Yibao Li[1], Changhoon Lee[1,2] and Jung-Il Choi[1,*]

[1]*Department of Computational Science and Engineering, Yonsei University, Seoul 120-749, Korea*
[2]*Department of Mechanical Engineering, Yonsei University, Seoul 120-749, Korea*

(Manuscript Received October 21, 2015; Revised December 15, 2015; Accepted December 20, 2015)

Abstract

We performed numerical simulations of blast wave propagations on surfaces by solving axisymmetric two-dimensional Euler equations. Assuming the initial stage of fireball at the breakaway point after an explosion, we investigated the effect of surface conditions considering surface convex or concave elements and thermal conditions on blast wave propagations near the ground surface. Parametric studies were performed by varying the geometrical factors of the surface element as well as thermal layer characteristics. We found that the peak overpressure near the ground zero was increased due to the surface elements, while modulations of the blast wave propagations were limited within a region for the surface elements. Because of the thermal layer, the precursor was formed in the propagations, which led to the attenuation of the peak overpressure on the ground surface.

Keywords: Blast wave propagation; Explosion; Peak overpressure; Obstacles; Thermal layer

1. Introduction

The flow field induced by the blast wave interacting with a surface is complicated due to shock wave reflections. Such an interaction often occurs in a high-energy explosion in chemical factories that can destroy buildings. Thus, a better understanding of the physical phenomena associated with blast waves is helpful in prediction of the blast damages after an accident.

For over half a century, many researchers [1-14] have investigated the blast wave propagations and interactions with a surface. When a shock perpendicularly impinges a planar surface, the reflected overpressure can be determined by a reflection factor that is defined as the ratio of the reflected and incident overpressures. Based on the Rankine-Hugoniot equations, it is known that the maximum reflection factor would reach eight for low to moderate overpressure shocks for an ambient air [2]. This is known as Regular reflection (RR). However, when the reflected shock is able to catch the incident shock, a single combined shock wave, known as Mach stem, is formed near the reflecting plane. This is known as Mach reflection (MR). Typically, the overpressure at the shock is about twice larger than that at the direct blast wave front [2]. After Ben-Dor's work [4], the shock wave reflection phenomenon has been characterized by four principal forms such as Regular reflection (RR), Single Mach reflection (SMR), transitional Mach reflection (TMR), and double Mach reflection (DMR). Later, Colella et al. [7] performed numerical simulations of a high-explosive-driven spherical blast-wave propagation on a surface to understand more details of the physical phenomenon of shock wave interaction with a surface. They found that even in RR region, the blast wave from the flat surface creates complex flow structures having multiple length scales and induces additional pressure pulses on the surface. Jiang et al. [13] numerically and experimentally investigated micro-blast-wave propagation on a flat surface. They clearly captured the formation of Mach stem as well as the triple point of Mach reflection in both micro-blast experiments and numerical simulations of the Navier-Stokes and Euler equations. Hu and Glass [14] theoretically analyzed blast wave propagation on a flat surface depending on Heights of burst (HOB). Liang et al. [5, 6] studied the four types of reflections of an unsteady cylindrical or spherical shock wave propagating over a wedge or an iso-thermal flat plate. They focused on transition phenomena of blast-wave reflection from the flat plate and the associated flow structure for strong blast waves.

Although it is important to understand comprehensive shock reflection phenomena even on an idealized surface, the properties of the reflecting surface should be taken into account for predictions of the blast damages after a real burst event. The most common real property is associated with surface rough elements (obstacle or terrain) on the ground, and the next one is a thermal heated layer on the ground resulting

*Corresponding author. Tel.: +82 2 2123 6129, Fax.: +82 2 2123 8194
E-mail address: jic@yonsei.ac.kr
This paper was presented at the AJK2015-FED, Seoul, Korea, July 2015.
† Recommended by Guest Editor Gihun Son and Hyoung-Gwon Choi

from a strong thermal radiation from the fireball [2]. From a macroscopic point of view, Dewey et al. [12] experimentally investigated the blast-wave interaction with a rough surface compared to the interaction with a smooth surface. They found that a smooth surface induces a stronger Mach stem and a higher triple-point trajectory compared to a rough surface. Needham [2] reported that a blast wave reflecting from a rough surface changes the character of both the geometry and the blast parameters of the reflected region of the wave. Moreover, the incident wave front reflects from each roughness element, which results in the stagnation of the near surface velocity and the enhancement of the overpressure. Ngo et al. [21] studied the effect of blast wave propagation on a building structure. They found that the incident peak overpressures are amplified by a reflection factor as the shock wave encounters an object or structure in its path. Smith and Rose [22] investigated blast wave propagation over an urban-like environment in both experimental and numerical approaches. This study indicated that both shielding and channeling effects in blast propagations through arrays of simple building structures should be considered in predicting the blast damages. Recently, Asl et al. [23] studied blast wave propagations interacting with a protection barrier (obstacle), and found that the protection barrier (obstacle) on the ground significantly alters the blast propagations and reduces possible blast damages, depending on the shape and size of the barrier. Therefore, more systematic studies on blast wave propagation considering its interaction with localized surface rough elements are needed for a better prediction of the blast damages.

On the other hand, after an explosion, a fireball with extremely high pressure and high temperature grows the time. When the pressure and thermal shock fronts of the fireball are separated, the radiation heat transfer inside the fireball is negligible for the blast wave propagations. However, due to the radiation, thermodynamic properties of the ambient air near the ground are significantly affected and a thermal heated layer is formed near the ground [15]. It is known that the influence of the layer on blast wave propagations leads to the formation of a precursor shock because the density in the thermal layer is lower than that in the atmosphere [15-18]. Since the previous studies were limited to a low-energy explosion, the role of the thermal layer on the blast wave propagation after a high-energy explosion is still unclear in the formation of a precursor shock.

The objective of the present study was to investigate the effect of geometric and thermal ground surface conditions on blast wave propagations after high-energy explosion using numerical simulations. Three kinds of geometric surface conditions, a flat surface, convex cylinder and concave cavity, were considered in order to characterize the propagations interacting with the ground surfaces. In particular, we performed parametric studies of geometric surface conditions on peak overpressure distributions along the distance from ground zero. The effect of thermal layer on the propagations was investigated by considering a low density (or heated) layer near the ground surface. Details of a precursor formation due to the thermal layer were discussed. The role of the thermal layer in the blast damages was also investigated through peak overpressure.

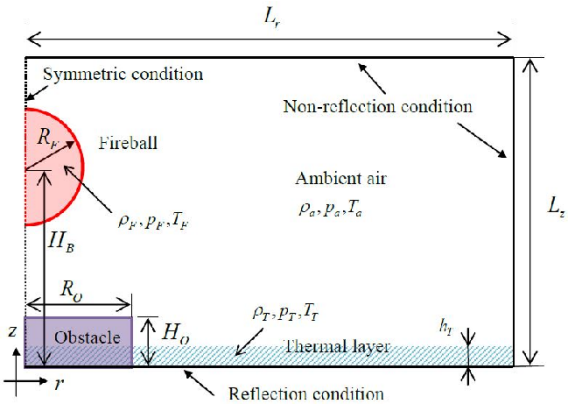

Fig. 1. Schematic diagram of a computational domain with initial and boundary conditions.

2. Numerical methods

We considered two-dimensional axisymmetric compressible inviscid flows for blast wave propagations interacting with ground surface. For the time-dependent compressible flows, the Euler equations are solved based on the cell-averaged finite volume method. The dimensionless hyperbolic equations for mass, momentum and energy conservations can be written in a cylindrical coordinates (r,z) as:

$$\frac{\partial \mathbf{U}}{\partial t}+\frac{\partial \mathbf{F}}{\partial r}+\frac{\partial \mathbf{G}}{\partial z}+\frac{\mathbf{S}}{r}=0\,, \tag{1}$$

where $\mathbf{U}$, $\mathbf{F}$, $\mathbf{G}$ and $\mathbf{S}$ are the vectors of conserved variables and fluxes in each direction, and source, given respectively by

$$\begin{aligned}\mathbf{U}&=\left(\rho \quad \rho u \quad \rho v \quad E\right)^T\\ \mathbf{F}&=\left(\rho u \quad \rho u^2+p \quad \rho uv \quad u(E+p)\right)^T\\ \mathbf{G}&=\left(\rho v \quad \rho uv \quad \rho v^2+p \quad v\left(E+p\right)\right)^T\\ \mathbf{S}&=\left(\rho u \quad \rho u^2 \quad \rho uv \quad u\left(E+p\right)\right)^T\end{aligned}\,. \tag{2}$$

Here, u and v represent velocity components in r and z direction, respectively, and ρ is air density, and E is the total energy. The air is assumed to be ideal gas having constant specific heat ratio $\gamma = 1.4$ and the specific gas constant $R = 287.058$ J/kg/K. The equation of state for the perfect gas is given as

$$p=\left(\gamma-1\right)\rho e\,, \tag{3}$$

where e is the specific internal energy. The total energy E

is defined as

$$E = \frac{p}{\gamma - 1} + \frac{1}{2}\rho\left(u^2 + v^2\right). \quad (4)$$

The governing equations for blast wave propagations are solved by using approximate Riemann solvers based on Roe's flux vector splitting scheme [19] coupled with a second-order TVD Runge-Kutta time integration scheme. For shock capturing, inviscid fluxes are discretized using a variant of the Piecewise parabolic method (PPM) [20].

Fig. 1 illustrates the computation domain for the present study. The initial conditions for the fireball were determined by the condition at the time when the pressure and thermal shock fronts are separated so that the radiation heat transport is negligible, which is known as a breakaway point [1, 2]. The initial conditions can be estimated based on solutions from radiation hydrodynamic equations. However, in this study we assumed that at the initial stage the flow variables such as pressure, density and temperature are constant within the fireball having the explosion total energy, which is similar to Glasstone and Dolan [1]. Based on 20 kTon explosion at the height of burst $H_B = 500$ m, we assumed that the radius of the fireball is $R_F = 110$ m, temperature is $T_F = 8000$ K and density is $\rho_F = 2.711$ kg/m^3 [1], while the ambient conditions are defined as $P_a = 101.325$ kPa, $T_a = 273$ K and $\rho_a = 1.293$ kg/m^3. The initial states of the fireball and ambient air are considered as still air. The reflection boundary condition is imposed on the ground and obstacle surfaces, while the non-reflection boundary condition is specified at the top and outer boundaries. Since the blast wave interactions with obstacles are primarily concerned in this study, the radius and height of the computation domain is set as 1 km × 1 km considering the region of interest. As a grid convergence study for blast wave propagation on the flat surface, we consider three different uniform grids (200×200, 300×300 and 400×400). The test confirmed that a 400×400 uniform grid is enough to provide accurate peak overpressure distributions compared to those of Glasstone and Dolan [1]. In this study, a 400×400 uniform grid was used for all simulations. The computation time step was set to 10^{-4} seconds.

3. Results

3.1 Blast wave propagation on flat surface

To understand basic flow physics for blast wave interaction with a surface, we investigated the evolutions of pressure waves over a flat surface after a high explosion in air. Fig. 2 shows pressure contours at different time instants. A highly pressurized region inside the fireball at the breakaway point is shown in Fig. 2(a). The formation of the Regular reflected (RR) waves is clearly captured in Fig. 2(b) when the incident blast wave from an explosion strikes the surface. As shown in Fig. 2(c), the steeper front of the reflected wave is traveling faster than the incident wave and is overtaking, resulting in a single combined shock such as Mach reflection (MR). The high pressure is found at the triple point. As shown in Fig. 2(d), the reflected wave near the ground has overtaken and fused with the incident wave to form a single front, which indicates a Mach stem [1, 2]. The present results clearly show the triple point at which the incident wave, reflected wave, and Mach front meet [1].

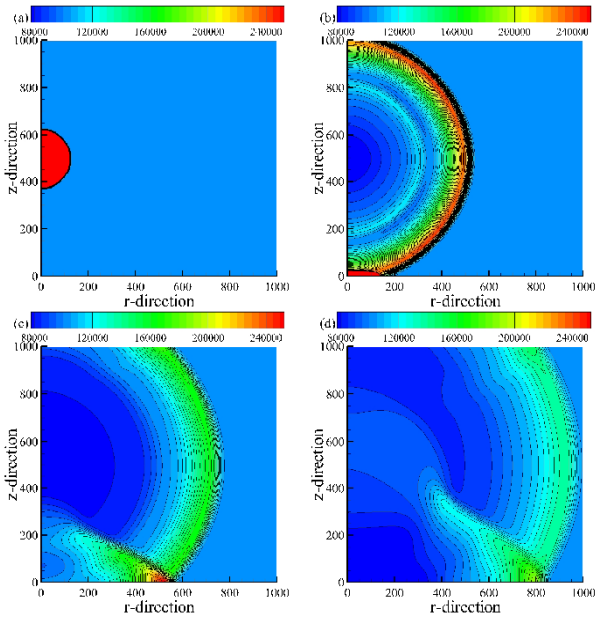

Fig. 2. Pressure contours for blast wave propagations on the flat surface at t = 0, 0.508, 1.008 and 1.498 seconds.

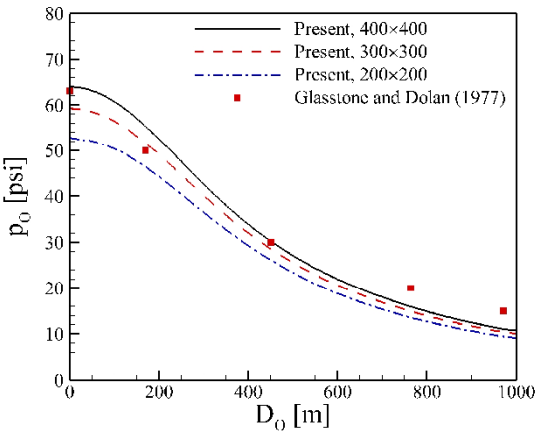

Fig. 3. Time histories of wall pressure on the flat surface at several downstream locations from the ground zero.

Fig. 3 shows the pressure variation with respect to time at several downstream locations from the ground zero. Note that D_O indicates the distance from the ground zero. At ground zero, the first shock wave induces an abrupt increment in the overpressure p_o to about 64 psi at t = 0.6 seconds when the first shock wave touches the ground surface. Following expansion waves cause a rapid decrease of the pressure. The overpressure decreases to about -5 psi at t = 1.8 seconds. Later, the pressure recovers to the ambient conditions after t = 3

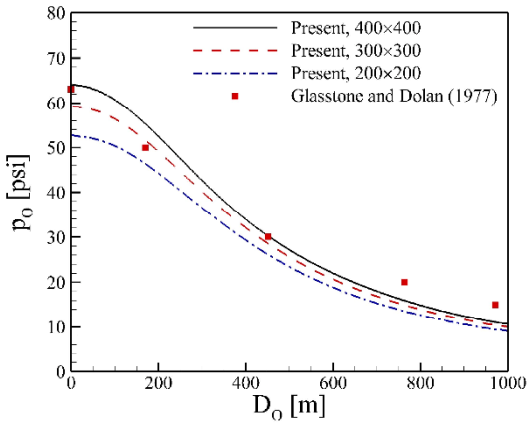

Fig. 4. Distributions of peak overpressure on the flat surface along the downstream locations from the ground zero.

seconds. A general trend of the pressure variations at other downstream locations is similar to the pressure at ground zero. For further downstream locations from ground zero, the peak overpressure decreases and the arrival time of the first shock wave becomes longer. Fig. 4 indicates that the numerical results for the peak overpressure distribution in the present study are in good agreement with those of Glasston and Dolan [1].

3.2 Effect of obstacles on blast wave propagation

To assess the effect of rough elements (obstacle or hole) on the blast wave propagations on the ground surface, we performed numerical simulations of the propagations considering various geometric configurations of the elements. The geometric configurations of cylinder-shaped obstacle (convex elements) and cylindrical cavity (concave elements) with various radius R_O, and height H_O (or depth) are as listed in Table 1. Note that a negative value of H_O indicates the depth for the cavity. The values of the peak overpressure p_o at the ground zero for each case are also listed in Table 1. For all cases of the convex obstacle, the peak overpressure at ground zero is higher than that for the flat surface. This is because the pressure shock touches the convex obstacle at an earlier time than the flat surface case. The overpressure increases with the increment of the obstacle height, while it is not sensitive to the radius of the cylindrical obstacle. But, when the obstacle height is equivalent to 20% of HOB, the peak overpressure is about two times higher than that of the flat surface. For a deeper and wider cavity, the peak overpressure at the ground zero is lower than that of the flat surface. The maximum reduction of the peak overpressure due to the cavity is about 30%. Interestingly, for a narrow cavity, the peak overpressure is higher than that for the flat surface, regardless of the radius of the cavity. This might be related to the shielding and channeling effects observed in Smith and Rose [22] for blast wave propagations in an urban-like environment, while it is expected that the pressure shock front containing lower energy might touch the cavity at ground zero.

Fig. 5 shows snapshots of pressure fields over three different surfaces at several time instants after 20 kTon burst at $H_B = 500$ m. For a comparison of pressure evolutions, we considered blast wave propagation on a flat surface, on a surface with a convex obstacle modeled by a cylinder with radius of 50 m and height of 50 m, and on a surface with a cavity of the same size as the convex cylinder. Before the first pressure shock shown in Fig. 5(a) touches the flat surface at t = 0.5016 seconds, Fig. 5(b) indicates that the first shock has already been reflected from the convex obstacle and moves toward the center of burst. However, the first shock does not reach to the bottom of the cavity as shown in Fig. 5(c). By t = 0.6187 seconds, a strong reflection region is found for the flat surface case. For the convex obstacle case, the reflected wave is clearly detached from the obstacle, while a high pressurized region is built in the cavity. At t = 0.7814 seconds, a weak Mach reflection is observed above the obstacle, while a strong pressure region still remains in the cavity. Except for the region near the obstacle or the cavity, the blast propagations for the three surfaces are similar to each other. At t = 1 second after the explosion, the triple point of the first shock front occurs at the same position for the three cases and the primary Mach stem is almost similar to each other. The cavity is completely de-pressurized and a mild rarefaction is observed above the cavity.

For a better understanding of blast wave interactions with the surface elements, time histories of the wall pressure at the ground zero and further downstream location for different surface conditions are shown in Fig. 6. Compared to evolutions of pressure wave on the flat surface in Fig. 3, the first

Table 1. Simulation conditions for rough elements on the ground surface and numerical results at the ground zero.

Case	Type	H_O / H_B	R_O / H_B	p_o	$\tilde{H}_B$	$\tilde{H}_B / H_B$	$\hat{p}_o$
1	Flat	0	0	64.1	500	1	63.1
2	Convex	0.2	0.05	123.7	400	0.8	114.2
3	Convex	0.2	0.1	124.1	400	0.8	114.2
4	Convex	0.2	0.2	124.1	400	0.8	114.2
5	Convex	0.1	0.05	86.2	450	0.9	84.3
6	Convex	0.1	0.1	86.8	450	0.9	84.3
7	Convex	0.1	0.2	86.8	450	0.9	84.3
8	Convex	0.05	0.05	73.2	425	0.95	73.4
9	Convex	0.05	0.1	73.9	425	0.95	73.4
10	Convex	0.05	0.2	73.9	425	0.95	73.4
11	Concave	-0.05	0.05	81.7	525	1.05	52.5
12	Concave	-0.05	0.1	63.9	525	1.05	52.5
13	Concave	-0.05	0.2	55.7	525	1.05	52.5
14	Concave	-0.1	0.05	70.7	550	1.1	46.9
15	Concave	-0.1	0.1	67.0	550	1.1	46.9
16	Concave	-0.1	0.2	49.0	550	1.1	46.9
17	Concave	-0.2	0.05	66.9	600	1.2	38.6
18	Concave	-0.2	0.1	59.7	600	1.2	38.6
19	Concave	-0.2	0.2	43.7	600	1.2	38.6

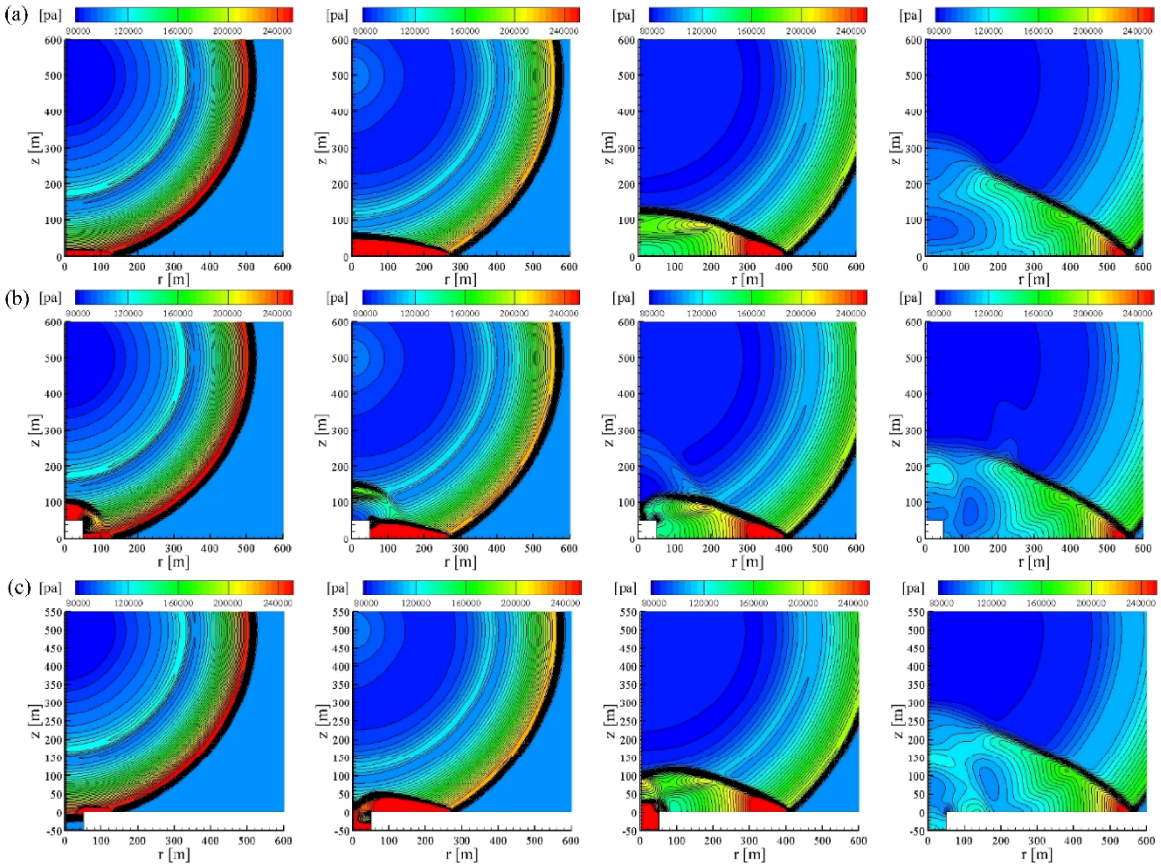

Fig. 5. Pressure contours for blast wave propagations on three surfaces at t = 0.5106, 0.6187, 0.7814 and 1.020 seconds for 20 kTon burst at H_B = 500 m: (a) Flat surface; (b) convex obstacle with $R_O = 0.1H_B$ and $H_O = 0.1H_B$; (c) concave cavity with $R_O = 0.1H_B$ and $H_O = -0.1H_B$.

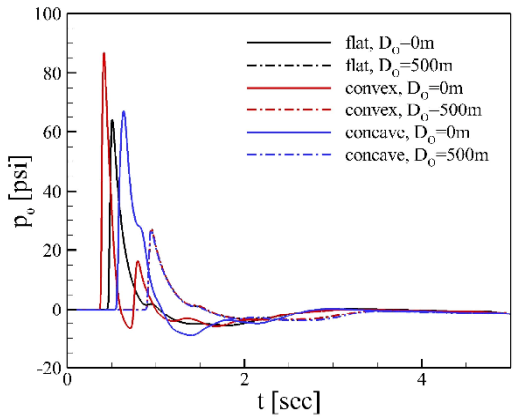

Fig. 6. Time histories of wall pressure on the flat surface and the surfaces with convex obstacle and concave cavity at the ground zero and a downstream location.

pressure shock propagation over the surface with an obstacle is slightly faster and the second pressure shock is detected at the ground zero, while the time history of wall pressure is almost similar to that on the flat surface. This implies that the shock propagations are modified only near the obstacle due to the presence of obstacle. For the cavity, the first pressure shock arrives later at ground zero compared to the flat surface case.

Fig. 7 shows the effect of geometric surface conditions on the peak overpressure distributions along the downstream locations. For a fixed height (or depth) of the obstacle (or cavity), the peak overpressure values are nearly constant within the region $D_O \le R_O$. A local minimum of the peak overpressure for each case is observed near the edge and corner of the obstacle and cavity, respectively. At far downstream locations $(D_O \ge 2R_O)$, the peak overpressure distributions are almost identical to the distribution for the flat surface case. For all cases of the convex obstacle with a certain height, the peak overpressure at the ground zero seems to be independent of the obstacle radius. However, for a given depth of cavity, the peak overpressure becomes higher as the cavity is smaller. Except for the wide cavity $(R_O = 0.5H_B)$, the peak overpressure at the ground zero is larger than that on the flat surface due to the surface elements. The effect of obstacle height and cavity depth on the peak overpressure distributions is shown in Fig. 7(b) for a fixed radius $(R_O = 0.1H_B)$ of obstacle and cavity. Except for the region near the obstacle or cavity, the peak overpressure distributions on the surfaces are almost similar to those on the flat surface. The peak overpressure at ground zero seems to be monotonically decreased with the increment of distance from the burst position to the surface of the obstacle and cavity.

One of important reasons for predicting blast wave propa-

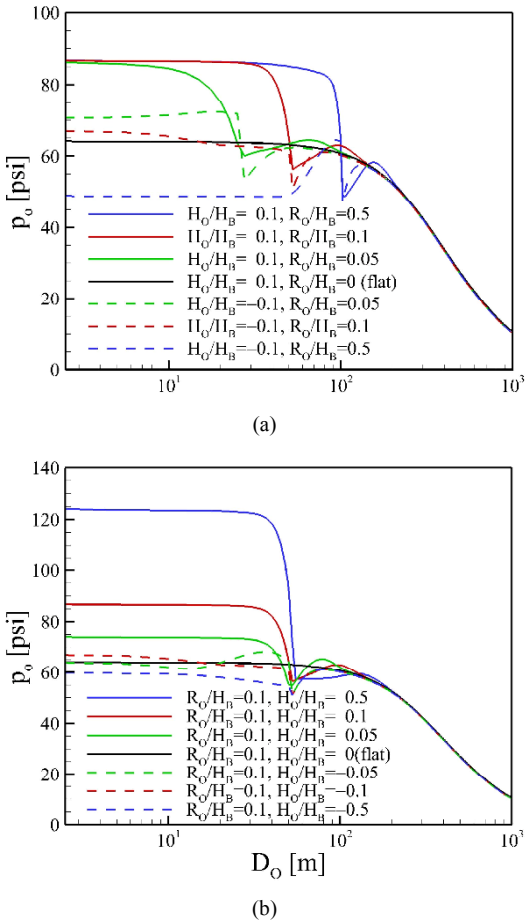

Fig. 7. Effect of obstacle (or cavity) size on peak overpressure distributions along the downstream locations from the ground zero: (a) Radius; (b) height (or depth) of obstacle or cavity.

gations after an explosion is to provide a reasonable estimation of the peak overpressure for the blast damage assessment, depending on blast parameters such as yield and distance. Under the assumption of detonation on an ideal flat surface, the peak overpressure can be obtained from the height of burst curves [1, 2]. For surfaces having rough elements such as obstacle and cavity, it is possible to estimate the peak overpressure based on an adjusted height of burst defined as $\tilde{H}_B = H_B - H_O$ from the height of burst curves. Fig. 8 shows the differences of the estimated peak overpressure from the numerical results. Note that $\hat{p}_o$ is estimated from the burst curves [1], as listed in Table 1. Except for the cases of the surface with a narrow cavity, the estimated peak overpressures from the curves show fairly good agreement with numerical simulation results within 15% error.

3.3 Effect of thermal layer on blast wave propagation

Due to the intense thermal radiation from the high-energy explosion impinging on a heat-absorbing surface such as desert or asphalt, a hot layer of air can be produced, which is known as thermal layer [1]. We modeled the thermal layer as

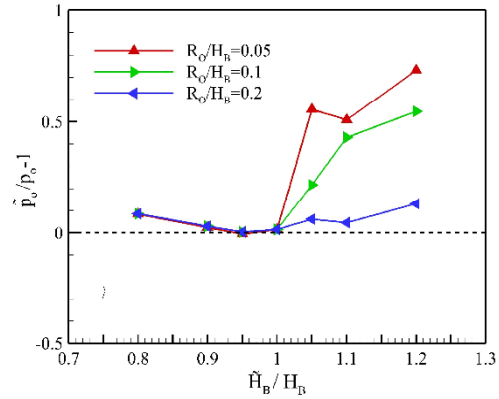

Fig. 8. Differences of the peak overpressure in between numerical simulation and estimation with adjusted height of burst for the surface with obstacles or hole.

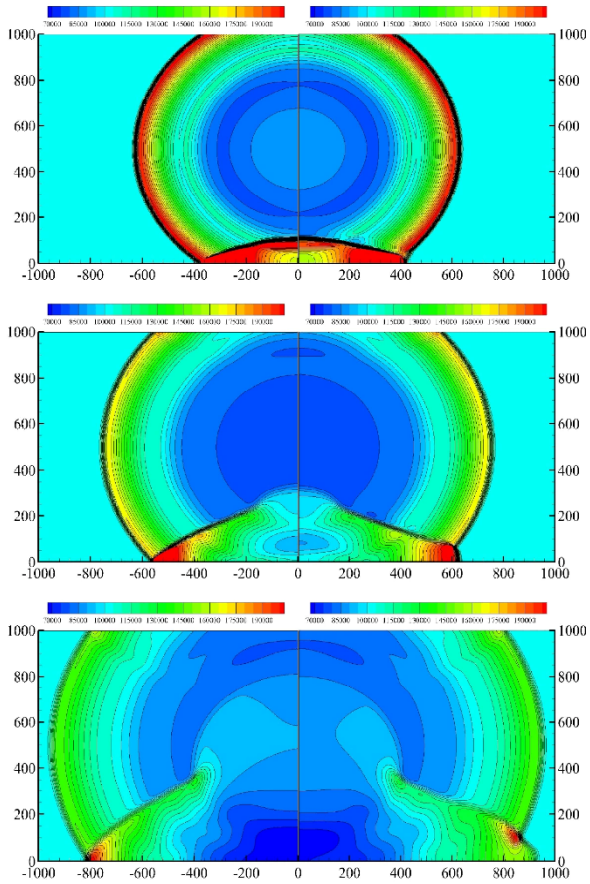

Fig. 9. Pressure contours for blast wave propagations on the flat surface without a thermal layer (left) and with a thermal layer (right) at t = 0.5, 1.0 and 1.5 seconds for 20 kT burst at $H_B = 500$ m.

a region where the temperature is higher than ambient air [15]. Fig. 9 shows the evolutions of the pressure wave propagations on the surface with or without thermal layer. The height of thermal layer is $h_T = 50\ m$ and the temperature in the layer is $T_T = 2.2T_a$. It is clearly seen that a precursor forms when pressure shock wave propagating through ambient air encounters the thermal layer. Precursor formation begins when the inci-

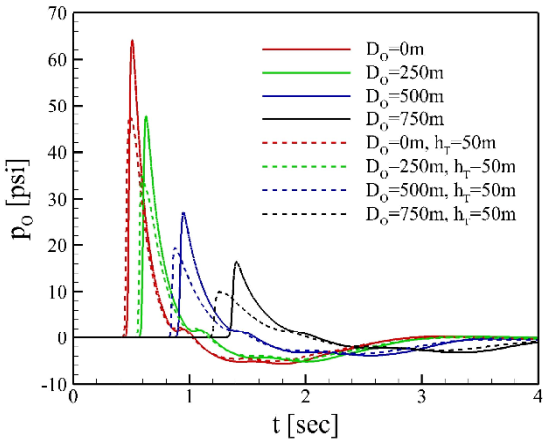

Fig. 10. Time histories of wall pressure on the flat surface with and without the thermal layer at several downstream locations from the ground zero for the case of 20 kTon with H_B = 500 m.

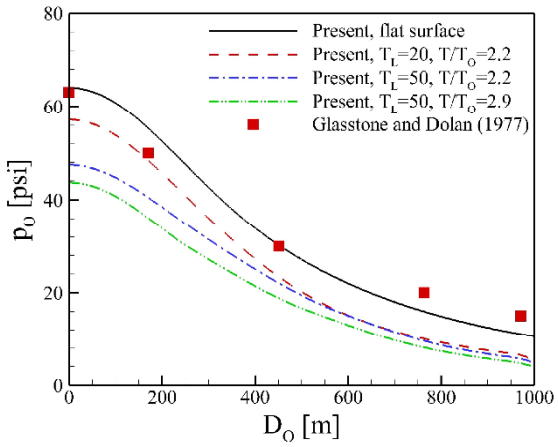

Fig. 11. Effect of thermal layers on the peak overpressure distributions along the downstream locations from the ground zero.

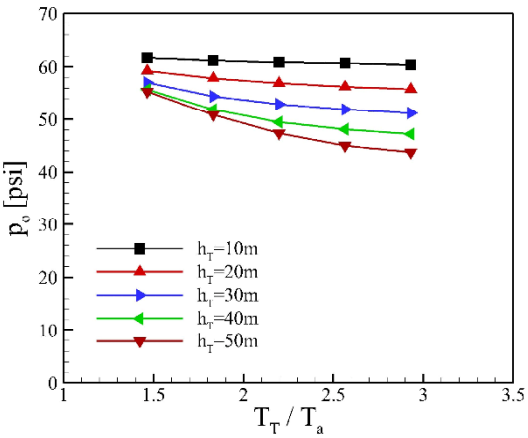

Fig. 12. Effect of thermal layers on the peak overpressure at the ground zero.

dent shock wave reflects into the layer at higher sound speed, creating a toe wave that accelerates ahead of the main shock. The toe wave pulls gas from behind the main shock, leading to the formation of vertical flow and an increased dynamic pressure within the layer. This drives another shock, the reflected precursor, that joins the incident and precursor shocks at a location called the triple point. High pressure behind the reflected precursor helps to sustain the gas flow, resulting in further growth of the toe wave.

Fig. 10 shows time histories of the wall pressure on surface from which the effect of thermal layer on the pressure wave propagations can be investigated. Compared to the temporal behavior of pressure wave propagation at the ground zero or near the ground zero (0 m and 250 m), the peak values of the pressure for the case of thermal layer are attenuated, but the incident time is similar to that for the case without the thermal layer. At further downstream locations from ground zero (500 m and 750 m), the peak incident time for the pressure is faster than that for the case without the thermal layer. While the overpressure characteristics are significantly modified by the thermal layer, the under-pressure characteristics are hardly changed by the thermal layer.

Fig. 11 shows the distributions of the peak overpressure on the surface with a thermal layer parametrized by its height and temperature. Due to the thermal layer, the peak overpressure is attenuated at all downstream locations compared to the peak overpressure on the flat surface without a thermal layer. This attenuation is more significant near ground zero. For a thicker or more heated layer, the attenuation of the peak overpressure is more pronounced. The attenuation due to the thermal layer might be related to the formation of the precursor shock near the ground surface. Results for the parametric studies on the effect of thermal layers on the peak overpressure are shown in Fig. 12. For a given thickness of the layer, the peak overpressure at the ground zero monotonically decreases with the increment of the temperature in the layer. Decreasing rates of the peak overpressure depending on the temperature conditions of the layers are increased when the layer becomes thicker.

4. Conclusions

We developed a two-dimensional axisymmetric inviscid compressible flow solver for simulating blast wave propagations on a ground surface. The present numerical method utilizes the approximate Riemann solvers based on Roe scheme [19] coupled with a second-order TVD Runge-Kutta time integration method. Inviscid fluxes are discretized by using a variant of PPM [20] for an accurate shock capturing. Numerical methods were validated through comparisons of the peak overpressure distributions on the flat surface along the downstream locations from the ground zero with those from the burst curves in Ref. [1]. Also, the present method clearly captures detailed shock phenomena for blast wave propagations on the flat surface after a high-energy explosion. To investigate the effect of surface elements such as convex cylinder and concave cavity on the blast wave propagations, we performed a systematic parametric study emphasizing its influ-

ence on the peak overpressure distributions. Due to the surface elements, the peak overpressure at the ground zero is increased, while at far downstream locations the peak overpressure distributions as well as temporal variations of the surface pressure are almost identical to those for the flat surface case. Note that scaling based on the adjusted height of burst for the peak overpressures at the ground zero enables to fairly accurately predict the peak overpressure from the burst curves [1]. Estimated peak overpressure at the ground zero shows less than 10% errors compared to the burst curves for the cases of $R_O/H_B \geq 0.2$. Thermal radiation emitted from the fireball causes heating and combustion of objects in the surrounding area. It is observed that after a high-energy explosion a thermal layer is formed near the ground surface depending on atmospheric visibility conditions [24]. To this end, we also investigated the effect of thermal layer, which is assumed to be a heated layer near the ground surface, on blast wave propagations. We found that a precursor shock is formed and the triple point moves away from the ground surface because the incident shock wave reflects into the thermal layer, creating a toe wave that accelerates ahead of the main shock. The corresponding peak overpressure at the ground zero is more attenuated for a thicker and more excessively heated layer. Although the results obtained in this study are limited to blast wave propagations near the ground zero for a surface with single object and generic thermal layer, better understanding of the effect of the surface conditions will benefit blast damage estimations over complex terrains after a high-energy explosion.

Acknowledgment

We gratefully acknowledge the supports of Agency for Defense Development and National Research Foundation of Korea (NRF-20151009350).

Nomenclature

U	: Variable vector
S	: Source vector
F,G	: Flux vectors in r and z direction
ρ	: Density
u,v	: Velocity in the r and z direction
p	: Pressure
E	: Total energy
R	: Specific gas constant
γ	: Ratio of specific heats
e	: Specific internal energy
K	: Kelvin temperature scale
H_B	: Height of burst (HOB)
R_F	: Radius of fireball
ρ_F	: Density of fireball
p_F	: Pressure of fireball
T_F	: Temperature of fireball
ρ_a	: Density of ambient air
p_a	: Pressure of ambient air
T_a	: Temperature of ambient air
ρ_T	: Density of thermal layer
p_T	: Pressure of thermal layer
T_T	: Temperature of thermal layer
h_T	: Thickness of thermal layer
H_O	: Height of obstacle or hole
R_O	: Radius of obstacle or hole
p_O	: Peak overpressure
D_O	: Distance from ground zero

References

[1] S. Glasstone and P. J. Dolan, *The effects of nuclear weapons*, US DoD (1977).

[2] C. E. Needham, *Blast waves*, Springer-Verlarg (2010).

[3] H. L. Brode, Numerical solution of spherical blast waves, *J. Appl. Phys.*, 26 (1955) 766-775.

[4] G. Ben-Dor, *Shock wave reflection phenomena*, Springer-Verlag, New York (1992).

[5] S.-M. Liang, J.-L. Hsu and J.-S. Wang, Numerical study of cylindrical blast-wave propagation and reflection, *AIAA J.*, 39 (2001) 1152-1158.

[6] S.-M. Liang, J.-S. Wang and H. Chen, Numerical study of spherical blast-wave propagation and reflection, *Shock Waves*, 12 (2002) 59-68.

[7] P. Colella, R. E. Ferguson, H. M. Glaz and A. L. Kuhl, Mach reflection from an HE-driven blast wave, *Dynamics of Explosions: Progress in Astronautics and Aeronautics 106* (ed. J.R. Bowen, J.-C. Leyer, R.I. Soloukhin), AIAA (1986) 388-421.

[8] D. K. Ofengeim and D. Drikakis, Simulation of blast wave propagation over a cylinder, *Shock Waves*, 7 (1997) 305-317.

[9] K. Kato, T. Aoki, S. Kubota and M. Yoshida, A numerical scheme for strong blast wave driven by explosion, *Int. J. Num. Mech. Fluids*, 51 (2006) 1335-1353.

[10] W. Peng, Z. Zhang, G. Gogos and G. Gzonas, Fluid structure interactions for blast wave mitigation, *J. Appl. Mech.*, 78 (2011) 031016, 1-8.

[11] O. Igra, G. Hu, J. Falcobitz and W. Heilig, Blast wave reflection from wedges, *J. of Fluid Engineering*, 125 (2003) 510-519.

[12] J. M. Dewey, D. J. McMillin, D. J. and D. F. Classen, Photogrammetry of spherical shocks reflected from real and ideal surfaces, *J. of Fluid Mechanics*, 81 (1977) 701-717.

[13] Z. Jiang, K. Takayama, K. P. B. Moosad, O. Onodera and M. Sun, Numerical and experimental study of a micro-blast wave generated by pulsed-laser beam focusing, *Shock Waves*, 8 (1998) 337-349.

[14] T. C. J. Hu and I. I. Glass, Blast wave reflection trajectories from a height of burst, *AIAA J.*, 24 (1986) 607-610.

[15] V. V. Shuvalov, Multi-dimensional hydrodynamic code SOVA for interfacial flows: Application to the thermal layer effect, *Shock Waves*, 9 (1999) 381-390.

[16] J. Grun, R. Burris, G. Joyce, S. Slinker, J. Huba, K. Evans, C. K. Manka, J. R. Barthel and J. W. Wiehe, Small-scale laboratory measurement and simulation of a thermal precursor shock,

J. Appl. Phys., 83 (1998) 2420-2427.
[17] V. A. Rybakov, I. V. Nemtchinov, V. V. Shuvalov, V. I. Artemiev and S. A. Medveduk, Mobilization of dust on the Mars surface by the impact of small cosmic bodies, *J. Georphys. Res.*, 102 (1997) 9211-9220.
[18] V. A. Andrushchenko, M. V. Meshcheryakov and L. A. Ghudov, Spherical shock wave reflection from a surface with a heated gas layer, *Fluid Dyn.*, 24 (1989) 607-613.
[19] P. L. Roe, Approximate Riemann solvers, parameter vector, and difference schemes, *J. Comp. Phys*., 43 (1981) 357-372.
[20] P. Colella and P. R. Woodward, The piecewise parabolic method (PPM) for gas-dynamical simulations, *J. Comp. Phys*., 54 (1984) 174-201.
[21] T. Ngo, P. Mendis, A. Gupta and J. Ramsay, Blast loading and blast effects on structures - An overview, *EJSE Special Issue: Loading on Structures* (2007) 78-91.
[22] P. D. Smith and T. A. Rose, Blast wave propagation in city streets-an overview, *Prog. Struct. Engng Mater.,* 8 (2006) 16-28.
[23] M. A. Asl and K. Kangarlou, Numerical simulation of barricades under blast wave propagation, *J. Appl. Environ. Biol. Sci.*, 4 (6) (2014) 72-79.
[24] H. Jung and W. Shim, Calculation of thermal fluence from extremely high-energy emission in air, *IEEE Trans. Nucl. Sci.*, 62 (3) (2015) 1395-1398.

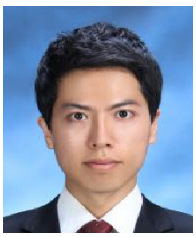

Seungho Song received his B.S. in Mechanical Engineering from Myongji University, Korea, in 2012. His M.S. in Mechanical Engineering is from Yonsei University, Korea, in 2014, where he is a graduate student. His research interest is in the area of compressible fluid dynamics.

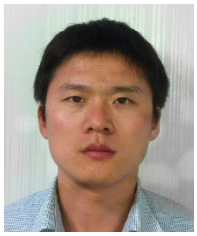

Yibao Li received the M.S. and Ph.D. in Applied Mathematics from Korea University, Korea, in 2011 and 2013, respectively. Currently, he is an Assistant Professor at the School of Mathematics and Statistics of Xi' an Jiaotong University, China. His research interests include image processing, phase field model, computational fluid dynamics and scientific computing.

Jung-Il Choi received the B.S., M.S. and Ph.D. in Mechanical Engineering from KAIST in 1994, 1996 and 2002, respectively. He is currently an Associate Professor of Computational Science and Engineering, Yonsei University, Korea. His research interests lie in the field of computational fluid dynamics and its application to various thermo-fluid engineering problems.

Changhoon Lee received his B.S. (1985) and M.S. (1987) from Seoul National University, Seoul, Korea and Ph.D. (1993) from UC Berkeley, USA., in Mechanical Engineering. He is a Professor in the Department of Computational Science & Engineering and Department of Mechanical Engineering, Yonsei University, Korea. His research interests include fundamentals of turbulence, particle-turbulence interaction, numerical algorithms, air pollution modeling and stochastic process.